

On muscle contraction mechanism

L. SKUBISZAK

*Institute of Biocybernetics and Biomedical Engineering, PAS
ul. Księcia Trojdena 4, 02-109 Warszawa, Poland
Ludmila.Skubiszak@ibib.waw.pl*

Mechanism of muscle contraction has been studied for a long time by different approaches. By the 1950s, this phenomenon was considered only at the macro level. Now, many interrelated mechanical, biophysical and biochemical events, occurring at the molecular level, are well known. To completely understand this mechanism the arrangement of the main proteins, actin and myosin, in the thin and thick filaments, respectively, has to be established. However, the available experimental methods do not allow to directly show the structural details of muscles. Consequently, main characteristics of the present-day models of muscle contraction have been deduced on the basis of different experimental data. As a remedy for coping with these differences, we have introduced a new approach based on computer simulation.

The aim of these lectures is to discuss the structure of vertebrate skeletal muscles at macro and micro levels. Two types of packing of myosin molecules within the thick filament and the models of muscle contraction as a consequence of the packing are analysed by computer simulation. These simulations are also available in the form of computer animation. Advantages of the new approach are proved by comparison of the obtained results with the experimental data by other authors.

1. Introduction

Mechanism of muscle contraction is one of the most enigmatic phenomena, though it has been studied for a long time. Such a situation is due to the complexity of the muscle structure, and many phenomena accompanying muscle contraction. These phenomena occur at both the macro- and micro- levels. However, the phenomena critical for understanding the muscle contraction occur on the molecular level. More precisely, insight into the actin-myosin interaction is a prerequisite to understanding the muscle contraction.

The present-day view on the muscle contraction mechanism is based on the so-called crossbridge-sliding model [1-4]. The main features of the model are:

- (1) the muscle contraction is a consequence of relative sliding of two sets of interdigitating filaments, thick ones, consisting of mainly myosin and thin ones, containing actin;
- (2) the force ensuring the sliding movement is associated with the cross-bridges cyclically protruding from the myosin filaments towards the surrounding actin filaments;
- (3) the crossbridges work in an oar-like manner, i.e. by bending the myosin molecule within two or three hinge domains;
- (4) the myofilaments themselves behave as inextensible structural elements;
- (5) force needed for the mechanical movement is converted from the chemical energy of the ATP hydrolysis (ATP – AdenosphineTriPhosphate);
- (6) the ATP hydrolysis is coupled with the actin-myosin interaction.

Only the first feature is assumed without objections because it was made on the basis of direct EM observations [5, 6]. The last two statements are confirmed only roughly by biochemical studies in different solutions (for a review see [2, 7]); however, the energy transition is not specified. The remaining statements are a consequence of general view on the manner of packing of the myosin molecules within the thick filament and the actin monomers within the thin filament. The oar-like action of the crossbridges presumes that the myosin molecules are erected along the filament axis, i.e. it is based on the concept of the so-called three-stranded model of vertebrate skeletal muscle thick filament (TS model). The postulate of the inextensibility means that the structure of myofilaments does not change during the muscle contraction. This means that the knowledge of the myofilament structure is crucial for understanding the muscle contraction mechanism. However, the structure of molecule packing within the myofilaments as well as the myosin crossbridge movement cannot be directly shown by any available experimental methods; these can be only deduced and simulated.

2. Structure of vertebrate skeletal muscle

It can be seen with the naked eye that muscle consists of a bundle of separate fibres, see Fig. 1. The number of fibres in a muscle is genetically determined, i.e. it does not depend on training. By using light microscopy, one can detect the next degree of complexity of muscles, namely that each of them is regularly striped and contains some other fibres called myofibrils. The striped structure of the skeletal muscle is clearly visible by electron microscopy. It turns out that each individual myofibril consists of some quasi-cells successively arranged along, and the membranes, separating the cells, bring about the muscle striping. These repeating units are called sarcomeres.

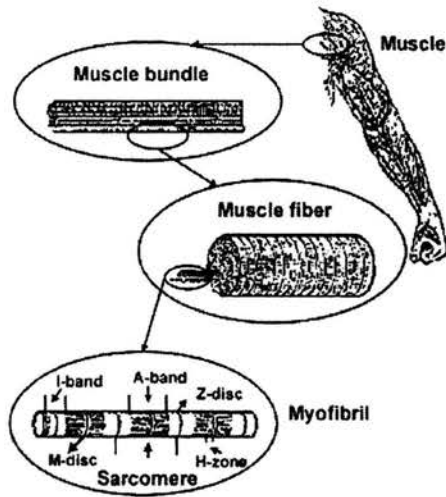


FIGURE 1. Diagrammatic representation of the skeletal muscle structure.

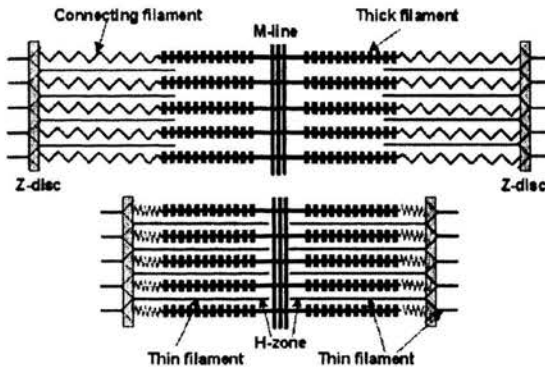


FIGURE 2. Scheme of the sarcomere contraction.

The sarcomere features turned out to be a milestone in understanding the cause of the muscle contraction. In the fifties of the last century [5, 6], the muscle was established to contract because of the contraction of the sarcomeres aligned along the fibre. Moreover, each sarcomere was shown [5, 6] to change its length during the muscle contraction due to sliding the thin filaments between thick ones, see Fig. 2. Much more later other filaments were found; for instance, such as connecting filaments [8-10], each of them linking the thick filament to the sarcomere end, i.e. to the Z-disk.

Specific features of the myofilaments determine the appearance of the individual myofibril as consisting of the alternating dark and light stripes, visible in the optical microscope. The thick filaments form the dark bands because they possess a sufficient molecular symmetry to rotate the plane of the polarised light; hence these bands are termed the A-bands (anisotropic bands). The thin filaments are linked to the Z-disc in such a way that on the opposite sides of the Z-disc the filaments are oriented in opposite directions. During muscle contraction, the free ends of thin filaments, oriented in the opposite directions stop short of the sarcomere middle, termed the M-line. The region divided by the Z-disc, from the margin of one A-band to the next one, does not rotate the plane of the polarised light. This area is termed the I-band (isotropic band). Then, the extent of the thick filaments is represented by the A-band; the extent of the thin filaments is represented by the I-band + A-band. At the centre of the A-band there is a band looking in electron microscopy as a brighter area; it is termed the H-zone. The M-line, looking as a thin dark line, is at the centre of the H-zone. The A-band length is about $1.6 \mu\text{m}$, the H-zone is about $0.13 - 0.16 \mu\text{m}$, the M-line is about $0.1 \mu\text{m}$ and the Z-disc is $0.1 - 0.3 \mu\text{m}$ [1, 3]. The other letters stem from German: "H" means Hellezone (bright zone), "Z" - Zwischenstreife (in-between band) and "M" from Mittellinie (midline).

3. New insight into the role of myofilaments in the muscle contraction

3.1. Relation between the thick filament structure and the cross-bridge action

In vertebrate striated muscles, most of the thick filament (80 – 90%) is made of myosin (between 270 and 300 myosin molecules); the remainder is made up of a number of accessory proteins (for a review see [11]). Because of this, the myosin features determine the thick filament features.

The myosin molecule has a very specific and complicated topology. It can be divided into two heads and a tail consisting of two specific subfragments, S2 and LMM, see Fig. 3.

The whole tail consists of about 1097 amino acid residues (for a review see [12]). The myosin tail from all the types of muscles consists of two α -helical heavy chains rounding one another into a left-handed coiled-coil [13-21]. At one of the ends, the tail diverges and, in conjunction with the light chains, separately fold to form two heads, see Fig. 4.

Each myosin head, according to the crystal structure [23], is "a comma" shaped with a length of over 16.5 nm, see Fig. 4. The point of the comma

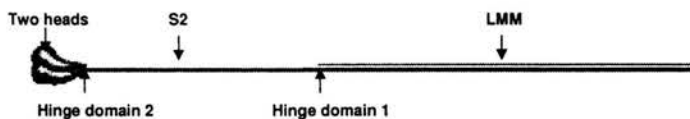


FIGURE 3. Myosin molecule modelled to a scale.

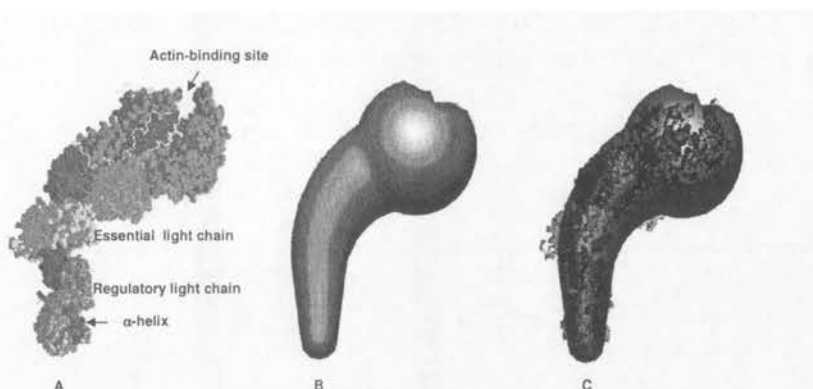


FIGURE 4. Myosin head models; A – the original model devised by Rayment [23] on the basis of myosin-head crystal structure; B – the model devised by Skubiszak [12] on the basis of parameters specified by Rayment; C – superimposition of the two models.

bending is about half way along the length. The thickest end is approximately 6.5 nm wide and 4.0 nm deep. In this part, at approximately one-third length of the thickest part from the head tip, the actin-binding site, looking as a prominent cleft, is located, and oppositely, there is the ATP-binding pocket. Along the narrow part, a long α -helix (approximately 8.5 nm long) extends down to the junction with the tail. This helix is enveloped by two kinds of light chains, essential and regulatory.

The classic crossbridge-sliding model [4, 24, 25] maintains that the myosin crossbridges play the main role in the contraction. Primarily, the bending of the myosin tail within the hinge domains 1 and 2 (Fig. 3) was taken into consideration (see Fig. 5). However, such a movement must involve quite significant changes in the angles between the LMM and the S2 as well as between the S2 and the myosin head. According to experimental data, these angles are much smaller (for a discussion see [26]). Moreover, if the force is generated only by the crossbridge rotation, the mutual displacement of the myofilaments and the velocity of their movement should be proportional to the number of the myosin crossbridges. However, it is true only for the isometric contraction when the servomechanism is applied (for a discussion see [3]).

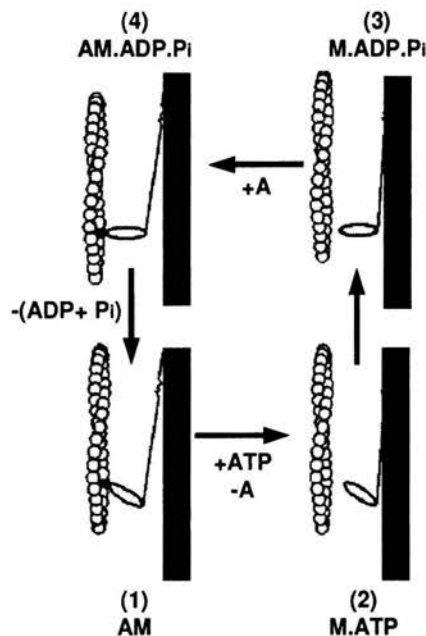


FIGURE 5. Oar-like movement of the myosin crossbridge. The crossbridge consists of the head linked to the S2 part of the myosin tail. The subfragments S2 and LMM both are straight. The LMM, lying parallel to the filament axis, makes up the filament backbone. The S2 rotates relative to the LMM, and the head rotates relative to the S2. Scheme of coupling of the mechanical events with the chemical events (e.g. ATP hydrolysis) is taken from [4].

As it was mentioned in the Introduction, the original hypothesis of the oar-like action of the myosin crossbridges [24,25] presume the parallel configuration of the myosin tails (see Fig. 5). Such a concept was introduced on the basis of different myosin derivative paracrystals structures observed by EM. Later on, the 0.51 nm meridional reflection observed in the high-angle X-ray diffraction patterns of vertebrate skeletal muscles was considered as a strong argument for the parallel arrangement of the coiled-coil α -helices with the pitch of 0.54 nm (for a review see [12]).

In the nineties of the last century, the so-called lever-arm model of muscle contraction has appeared (for a review see [4, 27-30]). According to this model, the force generation is associated with rotation of the neck domain of the myosin head relative to the motor domain (see Fig. 6); i.e. a new hinge domain, within the myosin head, has been added. However, the lever-arm model, as an addendum to the crossbridge-sliding model, is also insufficient to describe all the aspects of the muscle contraction mechanism.

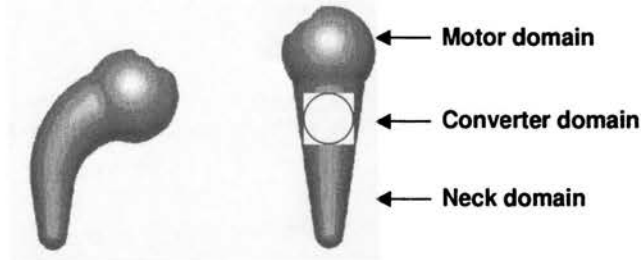


FIGURE 6. Lever-arm model of the muscle contraction. Myosin head bends due to conformational change within the so-called converter domain.

A 70° change of the angle between the neck and motor domains occurring as a consequence of conformational changes in the motor domain coupled with the type of nucleotide bind to the myosin head has been considered as a strong argument for the lever-arm model [31-33]. However, the needed conformational changes was observed after using molecular manipulation of the head, e.g. by removing existing reactive cysteines and placing new ones [34]. Moreover, three distinct states of the molecular motor was observed under three different circumstances. The next weakness of the lever-arm model consists in the fact that both the displacement and the velocity of the F-actin filament are not proportional to the length of the neck domain [35-38].

By the analysis of various modes of the myosin tail arrangements we have concluded [11, 12] that the tube-like appearance of the thick filament visible by EM (i.e. a very small inner hole, a quite massive wall and all arrangement of the myosin heads on the filament surface) could be modelled only for the twisted configuration of myosin tails; i.e. the tails should be twisted and not erected along the filament axis. Chew and Squire [39] have taken advantage of idea, but the degree of the tail twisting they took so small (within 1 – 3 degrees) that the tails look as if it be erected. The crossbridge action was similar to the crossbridge-sliding model (see Figs. 5 and 6).

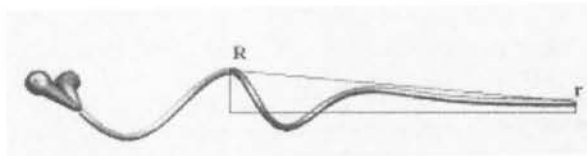


FIGURE 7. Twisted configuration of myosin tail used for modelling the complete bipolar structure of the thick filament (see Fig. 8). (The specific parts of the myosin are represented in the same way as in Fig. 3.)

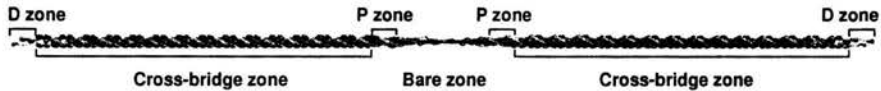


FIGURE 8. The complete bipolar model of the vertebrate skeletal muscle thick filament (called the CB model) generated from individual myosin molecules. The modelling is performed to a scale [12]. In the relaxed muscle, i.e. when all myosin heads lie on the filament surface, the filament appears as a bipolar rope with the central zone, two striping zones, and two sharpened flanks. The distribution of electrostatic charges along each myosin tail with a period of about 14.3 nm leads to the electrostatic attraction between the tails within the thick filament backbone [22]. Due to this feature, the thick filament possesses the specific axial period of 14.3 nm. The prominent, right-handed helical stripes uniformly extend across both arms of the filament with an axial interval of about 43 nm. Inclination of the helical stripes in the two polar halves are identical, of about 68° relatively to the normal to the filament axis. Along each helical stripe there are 4 or 5 well-marked clusters distributed axially about 14.3 nm apart. Each cluster reflects the pair of myosin heads and the helical striping is determined by the arrangement of the myosin heads on the filament surface. Due to the opposite orientation of the myosin tails in the central zone, the latter zone appears as being without the heads; so it is usually called the bare zone.

We have proposed quite a strong twisting, in particular that of the S2 part of the myosin tail (see Figs. 7 and 8). In consequence, each crossbridge possess a stiffness indispensable for action (see below). The new configuration of the myosin tail leads to a new action of the crossbridge; each of them unwraps from the filament surface and moves towards one of the surrounding thin filaments along a helical path (see Fig. 9).

The helical path for myosin tail arrangement shown in Fig. 7 we have accepted as optimal since it allows computation of the complete bipolar model of the vertebrate skeletal thick filament (see Fig. 8), the appearance and dimensions of which are consistent with the relevant experimental data [12, 40].

From the point of view of the new way of the crossbridge action the following experimental facts can be understood:

- (1) the behaviour of muscle as a viscoelastic medium;
- (2) the generation by muscle of not only the axial force but also radial;
- (3) the high stereospecificity of the actin-myosin interaction.

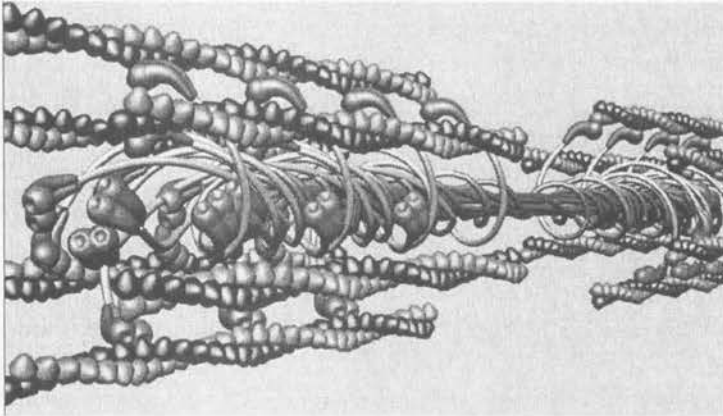


FIGURE 9. One of the phases of muscle contraction as a result of the crossbridge action by unwrapping. During the contraction, the stripes on the thick filament surface (Fig. 8) disappear because the crossbridges unwrap from the thick filament surface towards the surrounding thin filaments. Each crossbridge consists of two heads linked to the S2. In the two polar halves, the crossbridges are oppositely tilted in relation to the filament axis although the inclination of the helical paths is similar in the relaxed filament (see Fig. 8). In this way, the crossbridges from the two sarcomere halves pull off the thin filament sets towards the sarcomeres middle. The crossbridges appear only in the zones of the stripes; so, the bare-zone length is different in the relaxed muscle, during contraction, and in the rigor state, when all the crossbridges are connected with the surrounding thin filaments. Because the crossbridges work in sets of three, their arrangement in the gap between the thick and thin filaments within the hexagonal lattice of the sarcomere is different in different phases of the contraction.

The stereospecificity of the actin-myosin interaction means that during muscle contraction the myosin crossbridges should cyclically lead the actin-binding site situated on the myosin head to the myosin-binding site on the actin monomer. Because the dimension of each site is small in comparison to the whole globule, the stereospecificity imposes a very rigorous demand on the structural matching within the muscle sarcomere. The matching however impossible to understand on the basis of the contemporary concept of the thick filament symmetry.

The next problem consists in the mutual alignment of the crossbridges. It is well known that the myosin crossbridges are grouped in the so-called crowns. In vertebrate skeletal muscles, at each 14.3 nm axial level three crossbridges protrude from the thick filament backbone after muscle stimulation. Experimentally, it is not possible, however, to establish unequivocally the crossbridge crown configuration, i.e. the alignment of the three crossbridges in a crown and mutual rotation of the successive crowns.

According to the TS model, which has been proposed three decades ago [41, 42] and is still being prevalent [43, 44], each cross-bridge crown is symmetrical, i.e. the three cross-bridges are oriented at 120° , and the angle of the rotation between successive crowns is 40° . A structure of this type has been deduced on the basis of the following experimental observations:

- (1) the three-fold rotational symmetry of the whole thick filament;
- (2) the equilateral triangle visible in transverse view of the thick filament from the H-zone of the sarcomere;
- (3) the three helical paths symmetrically originating at an axial level and being of pitch 3×43 nm by which the myosin head distribution on the filament surface could be quite adequately extrapolated in the relaxed muscle.

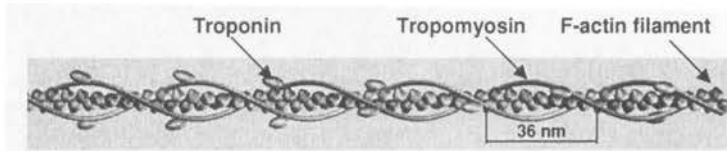


FIGURE 10. Thin filament structure of the vertebrate striated muscles. The modelling is performed to a scale. The F-actin filament is made up of individual actin monomers. Each monomer is generated as a ball covered by a cone. The monomers are arranged into a left-handed genetic helix with the axial translation of 2.75 nm and with the mutual rotation angle of 166.15° . Consequently, the filament looks like a two-start right-handed helix of two chains with the pitch of about 72 nm. Each of two chains contains 13 actin monomers per turn. Tropomyosin molecule is generated as a rope of length of 40 nm and diameter of 2 nm. The distance between the spots of the actin-tropomyosin connections correspond to the sets of 13 successive actin monomers. Troponin is represented as a globule of $44.8 \text{ nm} \times 86.9 \text{ nm}$. Each globule is tilted at the angle of 75° to the normal to the filament axis.

The analysis of the TS model performed by computer simulation [12, 26, 40] showed a number of its disadvantages. First, the symmetrical configuration of the crossbridge crowns results in cylindrical and not three-fold rotational symmetry of the whole filament. Second, in the TS model the cross-bridges protrude from the filament backbone along nine directions. However, because in the vertebrate skeletal muscle each thick filament is surrounded by six thin filaments and each thin filament by three thick filaments the crossbridges should protrude along the six directions. Third, one of the postulates of the classical crossbridge-sliding theory is that the myofilaments themselves, thick and thin, do not change their length during the mutual sliding, i.e. each of them behaves as an inextensible medium (see Fig. 2). Then, the structural matching required for precise contact between the actin and myosin is impossible to understand for two reasons. First, the thin fil-

ament is two-stranded and the thick filament of the TS-model type is three stranded. Second, the main periodic parts of the myofilaments are different. Axially, the myosin crossbridges occur at every 14.3 nm, but in the direction to the same thin filament – at every 43 nm. The actin monomers are axially 2.75 nm apart, but the myosin-binding sites are aligned along the same thick filament at every 36 nm (see Fig. 10).

The computer simulation has been devised so to analyse all reasonable manners of the myosin molecule arrangement within the thick filament model. The reason means that the distribution of all the myosin molecules on the filament surface ought to resemble that observed in the EM images of the relaxed thick filament (see the description in Fig. 8). Three of ten possible configurations have turned out to be adequate: one incorporated into the TS model and two new configurations, with the successive crowns rotated by 240° and the three cross-bridges in each crown aligned either at the angles 0° , 120° , and 180° or at 0° , 180° , and 240° . Such a configuration of the crossbridge crown, called asymmetrical as distinct from that incorporated into the TS model, results not only in the true three-fold rotational symmetry of the whole filament and correct number of the protruding crossbridges, but one of them, with the former alignment of the three crossbridges, leads to the optimal structural matching between the myofilaments during the muscle contraction simulated.

3.2. Thin filament structure

The structure of the vertebrate striated muscle thin filament is presently explored with the precision up to atomic distances (for a review see [28, 46-51]). Nevertheless, the present-day view on the thin filament structure is in principle the same as that proposed 40 years ago by Hanson and Lowy [52] and by Huxley and Brown [53]. The filament is composed of at least four types of proteins: actin, tropomyosin, troponin, and nebulin [for a review see [28, 45-51]]. The actin, in the form of globular G-actin monomers, assembles into filamentous F-actin; because of that the thin filament is often called the actin filament. Two other proteins, troponin (Tn) and tropomyosin (Tm), are usually called the regulatory proteins because they control the interaction of actin with myosin.

Each G-actin monomer, consisting of 375 amino acid residues can be described geometrically as a box or ellipsoid-like globule of $5.5 \times 5.5 \times 3.5$ nm. All the amino acid residues are grouped into four subdomains (see Fig. 11). The myosin-binding site is thought to be located in the subdomain-1, in the vicinity of the N- and C-termini.

The tropomyosin molecule is a two-chains, α -helical coiled-coil protein about 40 nm long [55]. The molecules link head-to-tail to form continuous strands along the actin filament. Each of the two tropomyosin strands fit loosely in the grooves between the two actin chains.

To each of the tropomyosin molecules a troponin molecule is attached. The Tn molecule, looking like a globule tethered to the tail, consists of three specific units [56]: troponin-C, TnC, troponin-I, TnI, and troponin-T, TnT (see Fig. 12). The tail, consisting of the longer part TnT, spans Tm towards the C-terminus; all the C-termini are oriented towards the Z-line.

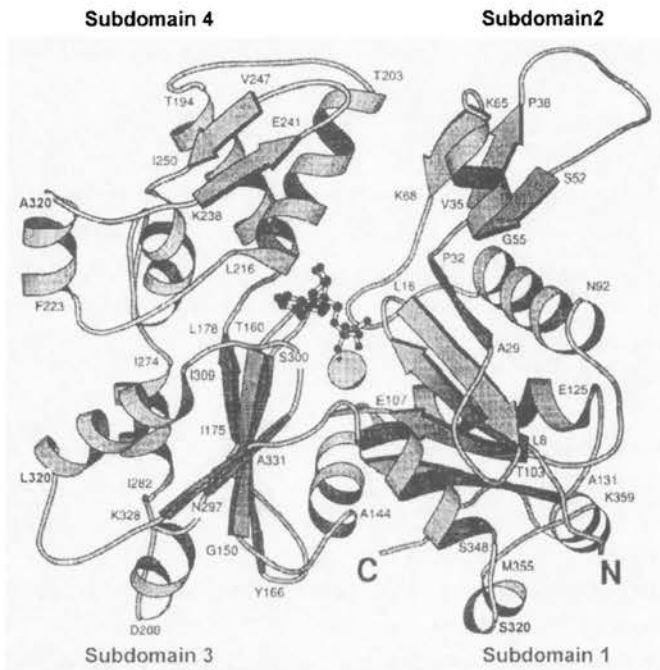


FIGURE 11. Diagrammatic representation of the G-actin structure, after [54].

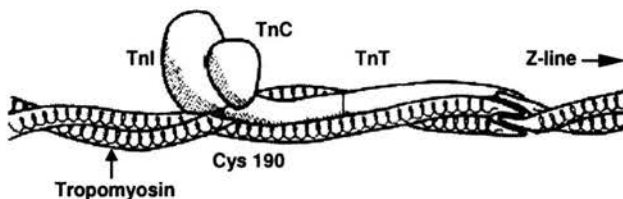


FIGURE 12. A diagram of the tropomyosin-troponin complex, after [57].

The role and the localisation of nebulin has not been clarified yet.

It is worth noting that the actin filament without its regulatory proteins is intrinsically active; i.e. it activates myosin ATPase and supports the force production (the so-called motility assay experiments) as well as the mutual movement of myofilaments.

3.3. The connecting filament

Microscopic studies carried out at the end of the 1980s have revealed that each thick filament is linked to the Z-disk by filaments consisting of titin molecules. Such filaments were called the connecting filaments (see Fig. 2), cf. [8-10].

Titin is the largest known protein. The titin molecule consisting of nearly 27 000 amino acids is $1.3\ \mu\text{m}$ long and 4 nm thick [10, 58-61], i.e. each molecule can pass through two distinct zones of sarcomere, the I- and A-bands spanning half the length of the sarcomere. This means that the A-band region of titin should contribute to the thick filament structure, and the I-band region appears as the connecting filament.

Biochemical studies have revealed that the A-band region of titin demonstrates approximately 44 nm super-repeat [10], i.e. this repeat is near the same as the repeat specific for the arrangement of myosin molecules within the thick filament [12]. Moreover, a regular arrangement of the super-repeats correlates well with the D-, C-, P- and M- zone architecture of the vertebrate thick filament [61, 62]. This molecule can interact with the thick filament components; it predominantly occurs with the LMM part of the myosin molecule [60, 61, 63]. The foregoing experimental evidences suggest that the main role of titin may consist in coordination of the myosin molecule association into thick filament.

Titin molecules could also contribute to the muscle contraction. It is well established that the A-band region is not extensible within the physiological sarcomere length range, whereas the I-band part reveals an elasticity [64-69]. Analysing the lengths of the sarcomere zones during the muscle contraction [70], we have concluded that the titin molecule has its native length $1.3\ \mu\text{m}$, at the sarcomere length of about $2.6\ \mu\text{m}$. Since the A-band part of the titin molecule is about $0.8\ \mu\text{m}$, the I-band part should be about $0.5\ \mu\text{m}$ long. The normal working range of sarcomere lengths is $2.1 - 2.4\ \mu\text{m}$. Thus, at the smallest sarcomere length, $1.6\ \mu\text{m}$, the titin molecule has to shrink up to 100%, and at the largest length, $3.6\ \mu\text{m}$, it has to stretch up to 100%. On the basis of such specific features of the titin molecule, it seems reasonable to conclude that the titin pulls the muscle sarcomere back, not only after being stretched (as it is thought), but also during the relaxation.

4. A new concept of muscle contraction mechanism

Experiments carried out during the last decade provided a number of facts crucial for understanding the muscle contraction mechanism. One of them is that the smallest set able to generate the force consists not of the two myofilaments, only of the F-actin filament and the separate myosin head. That suggests that in the muscle contraction the actin filament should play as active role as the myosin crossbridge [71, 72]. The features of the connecting filament mentioned above suggest in turn that this filament could also play an active role, especially during the muscle relaxation. In the classic, crossbridge-sliding model, only the myosin crossbridge is a powerful one. The experimental data, as well as the analysis performed by computer simulation shows clearly that an insight into the structure of the myofilaments, in particular into the thick filament, should be reinterpreted. We propose a new concept [26,72].

4.1. Description of the new concept

In the relaxed state of muscle, each myosin tail is twisted around the thick filament axis along a helical path, see Figs. 7 and 8. Therefore, all myosin heads lie on the thick filament surface. In the resting state, a number of the crossbridges, at the distance of 129.015 nm could be attached to the thin filaments since $14.335 \text{ nm} \times 9 = 129.015 \text{ nm}$ and $2.745 \text{ nm} \times 47 = 129.015 \text{ nm}$, where 14.335 nm and 2.745 nm are the axial translations between the cross-bridge crowns and the actin monomers, respectively.

Since the myosin tail is the α -helical coiled-coil, the twisted configuration should cause that each tail is in the state of increased potential energy; the myosin tail should possess a minimal potential energy when both myosin fragments, the LMM and the S2 are straight, see Fig. 3. The tail could be maintained at an increased energy by the electrostatic interactions with both the others tails and the accessory proteins contributing to the thick filament structure (for a discussion see [11]). Moreover, the myosin head, to which the ATP is associated, could be immobilized on the thick filament surface by interaction with the S2 and/or with the accessory proteins. There is a number of biochemical evidences for supporting such an assumption [11].

After muscle stimulation, the crossbridges begin cyclically unwrap from the thick filament surface and move towards the surrounding thin filaments. The crossbridges probably work in accordance with the scheme shown in Fig. 13.

Since the muscle is activated by an electric impulse, the myosin heads may detach from the thick filament surface due to a change in the distribution

of the electrostatic charge in the vicinity of the head-surface contact. The change could also be involved by the phase shift in the cyclic action of the crossbridges, see Figs. 9 and 13.

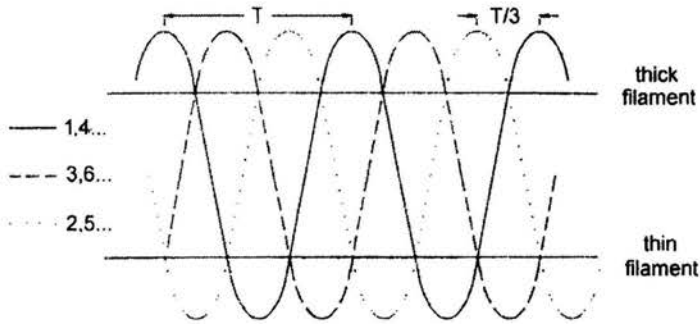


FIGURE 13. The cyclic action of the crossbridges belonging to three successive crowns. The three crossbridges belonging to the same crown as well as the crossbridge crowns being 43 nm apart work simultaneously. T is the period of action. The crossbridge crowns, being 14.335 nm apart, work with the phase shift $T/3$.

Meanwhile, the structure of the thin filament should change, in the first phase due to attaching of the Ca^{2+} to the TnC and in the second phase, due to interaction of the actin monomers with the myosin heads. We presume that the activation of the thin filament by the Ca ions consists in the change of the following dimensions: (see Fig. 14)

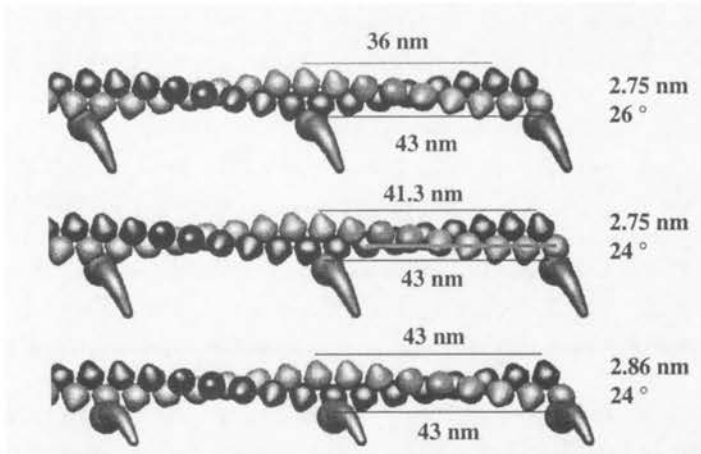


FIGURE 14. Simulation of the F-actin filament extension that probably appears after activation of the muscle.

- (1) the angle between the successive actin monomers within the genetic helix changes from 166.15° to 168° ;
- (2) the angle between the two chains of the superhelix changes from 26° to 24° .

The computer simulation revealed that the new dimensions lead to the change in position of the Tm-Tn complex often observed experimentally (for a discussion see below).

The electrostatic repulsion and the potential energy stored up within the S2 coiled-coil should bring about the crossbridge movement radially towards one of the six surrounding thin filaments and axially towards the sarcomere middle, see Fig. 9. Due to an electrostatic field existing around each thin filament, the crossbridge should get an additional acceleration. The energy reserve should decrease if the S2 straightens up. Yet, before reaching the steady-state, the crossbridge will hit into one of the surrounding thin filaments. Consequently, the remaining energy is transferred into the thin filament. If an actin-binding site on the myosin head associated with $\text{ADP}\cdot\text{P}_i$ hits precisely into the myosin-binding site on the actin monomer, the strong interaction between the actin monomer and the myosin head will be possible.

The actin-myosin interaction should involve a change in the interaction between the actin monomers adjacent to the actin-myosin interface. The computer simulation showed [71, 73] that if each myosin crossbridge causes a change in the axial translation between five successive actin monomers up to 2.867 nm, the structural matching required for the stereospecific interaction between the actin and myosin becomes possible. It is because of the following relations: $2.867 \text{ nm} \times 5 = 14.335 \text{ nm}$ and $24^\circ \times 5 = 120^\circ$, see Fig. 14. That means that each 14.335 nm shift of the thin filament should contain the $0.122 \times 5 \text{ nm}$ lengthening of the thin filament towards the middle of sarcomere.

Due to the interaction between the actin and the myosin, the myofilaments move together towards the middle of sarcomere. Consequently, the myosin crossbridge, immobilised on the actin monomer, changes its trajectory from helical, i.e. from that resulting in the S2 straightening, to that parallel to the long axis of the sarcomere. This should lead to generation of the tension within the S2 coiled-coil. Furthermore, the actin-myosin interaction affects the process of the ATP hydrolysis on the myosin head (see Figs. 5 and 15).

The dissociation of the $(\text{ADP}+\text{P}_i)$ complex from the myosin head should cause detachment of this head from the thin filament. Moreover, the conformational change within the thin filament in the vicinity of the actin-myosin contact should lead to a local change in the electrostatic field. In consequence,

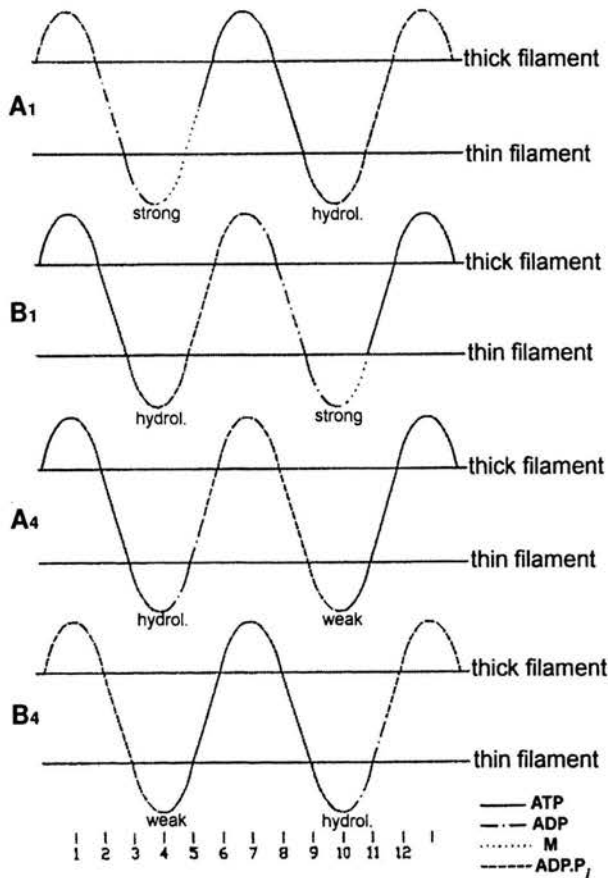


FIGURE 15. Cyclic action of the myosin crossbridges (Fig. 13) coupled with the cyclic process of the ATP hydrolysis.

due to the local electrostatic repulsion, the myosin head will detach from the thin filament, and due to the tension in the S2, the crossbridge will move back to the thick filament surface. The movement may be accelerated by the local electrostatic attraction from the thick filament.

The mechanism just described seems to be attractive since it helps in understanding a number of events observed experimentally but difficult to interpret from the point of view of the classic, crossbridge-sliding theory. First, the F-actin filament displacement observed in various motility experiments [31-33] should not always depend on the length of the neck domain of the myosin head [35-38]. Second, the relation between the force generated by the muscle and the number of the crossbridges should not be linear (see

Fig. 11.13 in [3]). Third, precise matching between the myofilaments insuring the stereospecific interaction between the actin monomer the myosin head could be achieved. Finally, the crossbridge movement along a helical path and the conformational changes within the thin filament should lead to the viscoelasticity [72] of the muscle sarcomere.

The mutual sliding of the myofilaments (thick and thin) should cause a stiffness within the connecting filaments. Therefore, the muscle relaxation will take place due to the potential energy stored within the titin molecules, creating the connecting filaments, as well as within the thin filament helix.

Thin filament extension caused by the change of mutual arrangement of the G-actin monomers (see Fig. 14) seems to be the only reasonable mechanism allowing to explain the movement of the Tm-Tn complex. The lateral movement of the tropomyosin strands towards the centre of the thin filament grooves was observed to be initiated by binding of calcium ions to troponin [46, 74-79]. On the basis of such observations, the so-called *steric blocking model* of the muscle contraction has been proposed (for a review see [79]). According to this model, the Tm-Tn complex physically blocks the myosin-binding sites on actin monomers in the resting state, and the shift exposes the sites for interaction. The cause of such a movement has not yet been clarified, but it is interesting that the event has never been associated with a shifting of the actin monomers. The legitimacy of the new hypothesis could be confirmed by calculation of the Fourier transforms for different phases of the muscle sarcomere contraction (see Fig. 16). The consistency of the redistribution of the reflections calculated and measured (Fig. 16) shows clearly that the cause is the structural changes within the thin filament and none of the perturbations within the myosin structure usually suggested by others authors.

5. Computer system MUSCLE

Studying the literature pertaining to the muscle structure and contraction, we have concluded [40] that the reconstruction methods usually applied for modelling of the muscle structure on the molecular level, especially those related to the thick filament structure, provide some ambiguity in the interpretation of experimental data. As a remedy we have proposed a new approach [12, 40, 81]. Our approach consists in the computer simulation of the muscle sarcomere from individual filaments, myosin and actin, and the filaments from individual molecules, myosin and actin, respectively. We emphasize that all elements are modelled to a scale.

The set of the computer programs devised we have called the system MUSCLE. We say system because it allows not only modelling with explor-

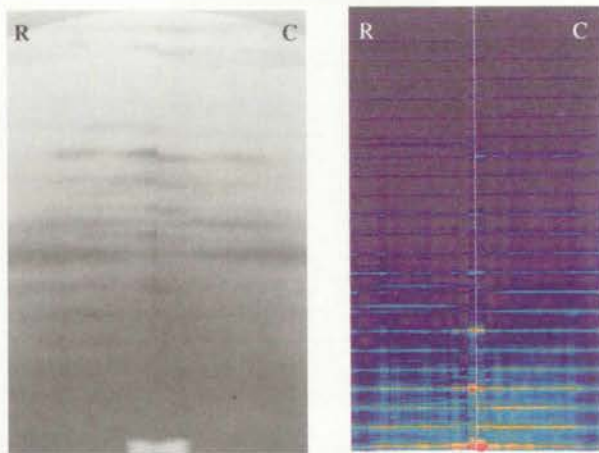


FIGURE 16. Comparison of the low-angle *X*-ray diffraction patterns obtained from the living muscle (left, from [80]) with that calculated for a bundle of filaments consisting of 7 thick and 6 thin ones (right); R – relaxed state; C – contraction.

ing varies geometrical parameters, but also verification of models by such experimental methods as EM and diffraction. Moreover, the system allows the creation of the animations of the molecule association into a filaments, as well as an animation of a muscle contraction.

As the main disadvantages of the reconstruction methods, routinely applied in modelling of the myofilament structure, two aspects are worth noting. First is the fact that they are based on electron micrographs, the resolution of which is not, however, sufficient to show all the details on the surface. Nothing can be inferred about the internal structure of a 3D sample. Consequently, in the case of the thick filament, there is no certainty even about the arrangement of the myosin heads on the filament surface. As to the internal structure of the myofilaments, none of the details can be revealed by the presently available experimental methods. Second disadvantage of the reconstruction methods consists in possibility to deliver only one solution.

The main advantage of our approach is that it allows to explore all reasonable manners of packing of the whole myosin molecule (see Fig. 3) within the whole, bipolar thick filament (see Figs. 8, 17 and 18A-18C). In the case of the thin filament, the arrangement of as the G-actin monomers as the Tm and Tn molecules can be examined in details (see Figs. 10 and 18D). By comparison of the computed models with the real structure the optimal parameters have been selected. On the basis of these parameters the complete bipolar structure of the vertebrate skeletal muscle thick filament have been for the first time modelled [40]. As so far, only a fragment of the polar zone of the filament have been reconstructed.

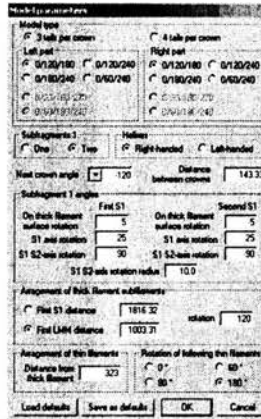


FIGURE 17. Window for selection of the parameters depicting the mutual arrangement of the myosin molecules within the thick filament and the myofilaments, thick and thin, within the muscle sarcomere. The values within the white windows are optional.

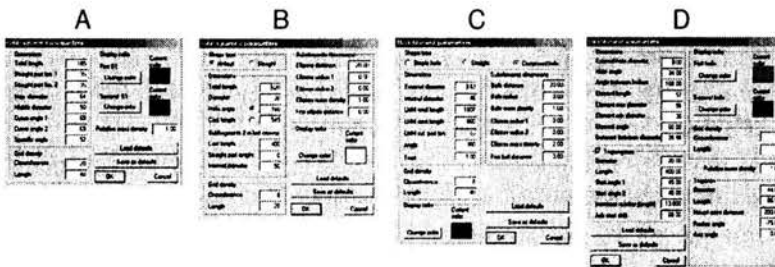


FIGURE 18. Windows for selection of the parameters describing (A-C) each of the four specific subfragments of myosin molecule (two heads, S2, and LMM, see Fig. 3 and (D) each actin monomer, tropomyosin molecule, and troponin molecule. Values within the white windows are optional. The dual components (e.g. two heads of the same myosin molecule, two fragments of the same myosin tail, neighbouring two actin monomers) are realised by attributing particular colour.

Experimentally measured dimensions of the specific parts of molecules as well as of the filaments are usually expressed in some ranges, see Tables 1 and 2 in [12]. It is clear that the analysis aimed at establishing optimal parameter values from the bulk of experimental data by a trial-and-error method is rather time-consuming. Implementation of a number of original and helpful options (see menus VIEW, CUT, and TRANSFORM in Fig. 19) allowed to make the system MUSCLE works quickly and is reliable.

To explore a mutual spatial arrangement between individual elements within the 3D sample, each model fragment can be zoomed, cut and measured

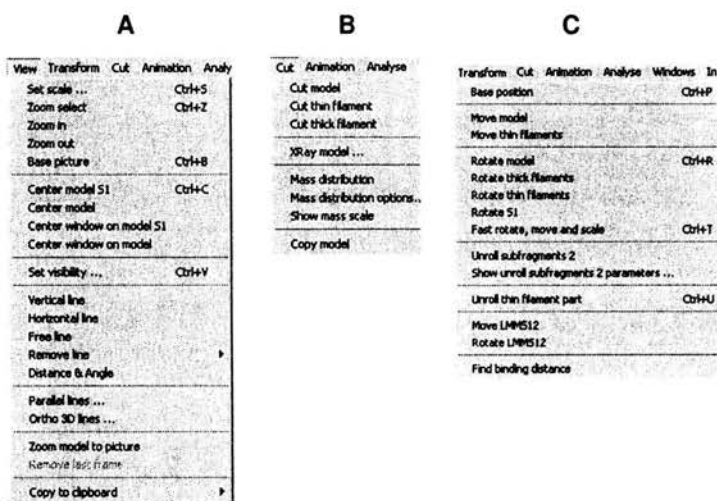


FIGURE 19. Windows *VIEW* (A), *CUT* (B) and *TRANSFORM* (C) useful for analysis of a chosen fragment of the model.

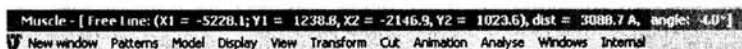


FIGURE 20. The line represents the ruler, the co-ordinates of which, length and inclination are automatically visualised in the upper line.

by a ruler with an accuracy of 0.01 nm, see Fig. 20. Moreover, each model fragment can be rotated and moved in three directions with resolution up to 1° and 0.1 nm, respectively, see Fig. 19C.

The whole model as well as its elements can be regenerated in a number of options (see Fig. 21, menu *DISPLAY*), and the picture can be printed, saved or copied to a new window or to the clipboard.

For a more accurate examination of different manners of myosin molecule packing, an original and quite helpful function has been devised [82]. It consists in summing up the pixels belonging to the model along particular lines going through the model perpendicularly to the plane parallel to the filament axis. In this way the sets of pixels form the 2D picture, which depicts the mass distribution along the chosen direction, see Fig. 22. This easy and quite fast simulation of the mass distribution allows for a direct verification of different manners of the myosin head arrangement on the filament surface by electron micrographs of separate thick filaments, see [40]. Moreover,

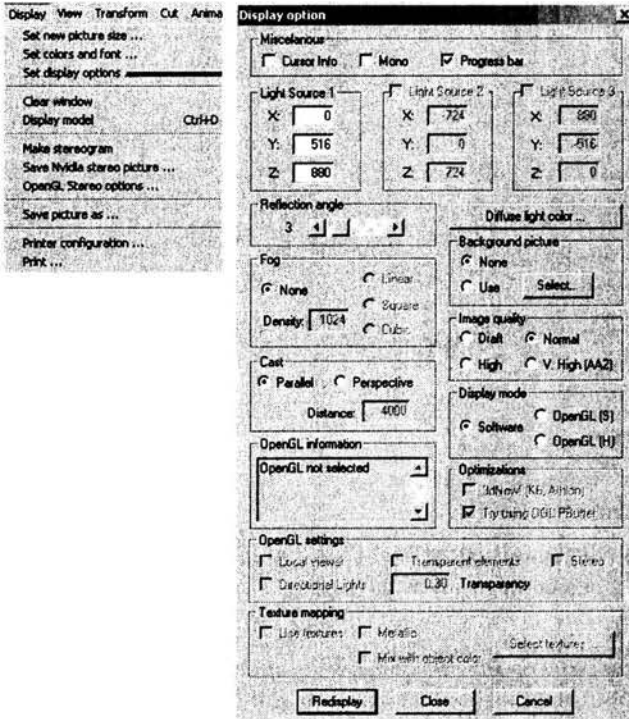


FIGURE 21. Window *DISPLAY*. The model can be shown in the parallel or perspective cast as well as in the stereo-pair view. To achieve a better 3D looking, the model can be lighted from one, two or three positions. There are four modes of graphic quality; the Draft and Normal modes are usually selected to speed up the model analysis; the High and Very High modes, by smoothing of edges, lead to considerable improvement of the model graphics. There is also a possibility to make different editor functions.

the calculation of the mass distribution along the filament axis provides a possibility for a direct examination of relations between the myosin molecule packing and the thick filament symmetry, see [40].

The 2D pictures depicting the mass distribution are used for the calculation of the Fourier transform, see [40]. Such an approach, based on the image processing procedure [84], is much faster and easier than that used so far and based on the equation of Klug et al. [85]. Moreover, it is worth noting that the resolution of the calculation depends on the precision of modelling; because of that at a proper scale it could give spectra not only better resembling those observed experimentally (see Fig. 23), but also reflecting much more details, in particular, if the spectrum is represented by a colour palette (compare Fig. 23 with Fig. 16).

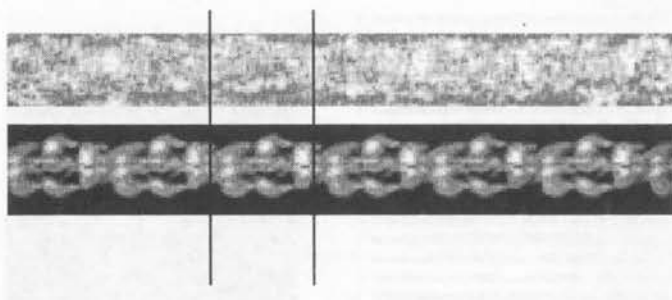


FIGURE 22. Mass distribution experimentally observed (upper line, from [83]) and simulated for the CB model (lower line).

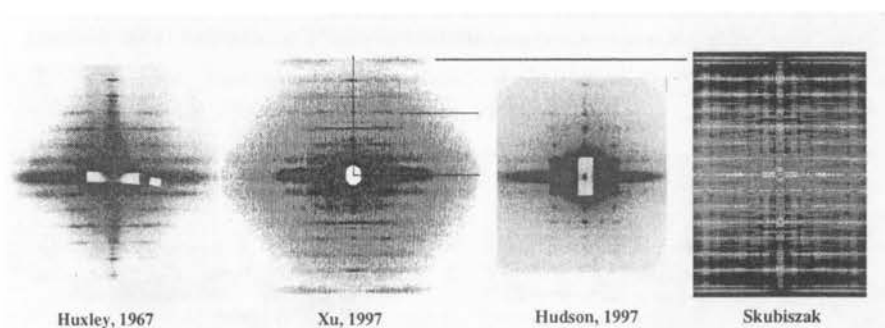


FIGURE 23. The Fourier spectrum calculated for the CB model (the right image) is compared with that calculated for the TS model by Hudson [88] (the second image from the right) as well as with the low-angle X-ray diffraction pattern measured for the living muscle by Huxley [53] and Xu [87] (the first and second images from the left, respectively).

The new approach provides unique possibility to analyse a number of controversial aspects. These are related to the following:

- (1) the model symmetry can be directly defined instead of introducing it *a priori*;
- (2) by consideration of particular structures (by using the option *VISIBILITY*, see Fig. 19), incorporation of the beam parameters into the calculation becomes unnecessary;
- (3) various physiological states of the muscle as well as various phases of the muscle contraction can be analysed (see Fig. 16). Moreover, the calculations for the model, in which particular elements are shown, justifies comparison of the Fourier spectra with the related diffraction patterns see, Figs. 23–25.

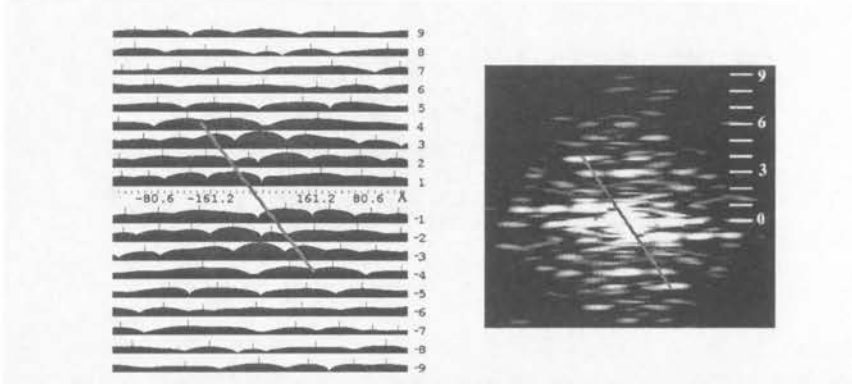


FIGURE 24. Comparison of the optical diffraction patterns. On the left, the Fourier transform calculated for a crossbridge fragment of the CB model. On the right, the patterns experimentally obtained for a separate thick filament, (after [86]).

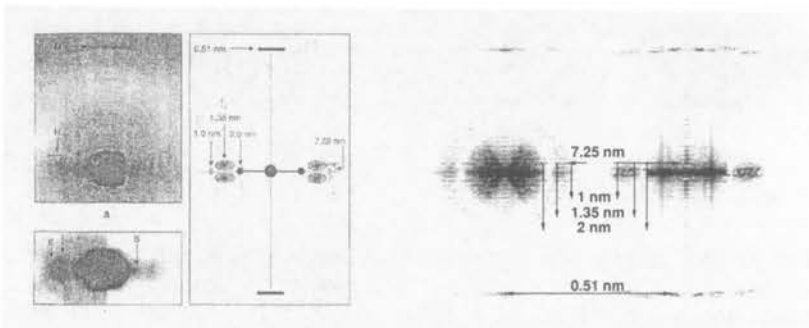


FIGURE 25. Comparison of the high-angle X-ray diffraction pattern (A, from [39]) with the Fourier transform (B) calculated for the filament backbone consisting of twisted LMM (left) and straight LMM arranged nearly parallel to the filament axis (right).

References

1. A. F. HUXLEY, Reflection on Muscle, *Princeton University Press*, Princeton, New Jersey, 1980.
2. R. COOKE, *The mechanism of muscle contraction*, CRC Crit. Rev. Biochem., Vol.21, pp.53-118, 1986.
3. G. H. POLLACK, In: *Muscle and Molecules. Uncovering the Principles of Biological Motion*, *Ebner and Sons Publishers*, Seattle, 1990.
4. M. A. GEEVES and K. C. HOLMES, Structural mechanism of muscle contraction, *Annu. Rev. Biochem.*, Vol.68, pp.687-728, 1999.
5. A. F. HUXLEY, Muscle structure and theories of contraction., *Prog. Biophys. Biophys. Chem.*, Vol.7, pp.255-318, 1957.

6. H. E. HUXLEY and J. HANSON, Preliminary observations on the structure of insect flight muscle, in S. Rhodin, (Ed.), *Proceedings of Conference on Electron Microscopy*, Stockholm, pp.202-204, 1957.
7. M. A. GEEVES, The actomyosin ATPase: a two-state system, *Philos. Trans. R. Soc. Lond. Biol. Sci.*, Vol.336, pp.63-70, 1992.
8. K. MARUYAMA, S. MATSUBARA, R. NATORI, Y. NONOMURA, S. K. OHASHI, F. MURAKAMI, S. HANDA, and G. EGUCHI, Connectin, an elastic protein of muscle: characterization and function, *J. Biochem.*, Vol.82, pp.317-337, 1977.
9. K. WANG, J. MCCLURE, and A. TU, Titin: major myofibrillar components of striated muscle, *Proc. Natl. Acad. Sci.*, USA, Vol.76, pp.3698-3702, 1979.
10. D. O. FÜRST, M. Osborn, R. Nave and K. Weber, The organization of titin filaments in the half-sarcomere revealed monoclonal antibodies in immunoelectron microscopy: A map of ten non-repetitive epitopes starting at Z line extends close to the M line, *J. Cell Biol.*, Vol.106, pp.1563-1572, 1988.
11. L. SKUBISZAK, Force generation in muscle: 1. Molecular organization in the thick filament, *Biocyb. Biomed. Engin.*, Vol.13, pp.75-96, 1993.
12. L. SKUBISZAK and L. KOWALCZYK, Myosin molecule packing within the vertebrate skeletal muscle thick filaments, A complete bipolar model, *Acta Biochim. Pol.*, Vol.49, pp.829-40, 2002.
13. M. SLAYTER and S. LOWEY, Structure of the myosin molecule as visualized by electron microscopy, *Proc. Natl. Acad. Sci. USA*, Vol.58, pp.1611-1618, 1967.
14. D. M. YOUNG, M. H. Blanchard and D. Brown, Selective nonenzymic cleavage of the myosin rod: Isolation of the coiled-coil α -rope section from the C-terminus of the molecule, *Proc. Natl. Acad. Sci. USA*, Vol.61, pp.1087-1094, 1968.
15. S. LOWEY, H. Slayter, A. Weeds and H. Baker, Substructure of the myosin molecule. 1. Subfragments of myosin by enzymic degradation, *J. Mol. Biol.*, Vol.42, pp.1-29, 1969.
16. A. G. WEEDS, and S. LOWEY, Substructure of the myosin molecule. II The light chains of myosin, *J. Mol. Biol.*, Vol.61, pp.701-725, 1971.
17. A. G. WEEDS and B. POPE, Studies on the chymotryptic digestion of myosin. Effect of divalent cations on proteolytic susceptibility, *J. Mol. Biol.*, Vol.11, pp.129-157, 1977.
18. A. ELLIOTT and G. OFFER, Shape and flexibility of the myosin molecule, *J. Mol. Biol.*, Vol.123, pp.505-519, 1978.
19. K. SUTOH, T. Karr and W. Harrington, Isolation and physico-chemical properties of a high molecular weight subfragment-2 of myosin, *J. Mol. Biol.*, Vol.126, pp.1-22, 1978.
20. T. Y. TSONG, S. Himmelfarb and W. F. Harrington, Stability and melting kinetics of structural domains in the myosin rod, *J. Mol. Biol.*, Vol.164, pp.431-450, 1983.
21. M. STEWART and P. EDWARDS, Length of myosin rod and its proteolytic fragments determined by electron microscopy, *FEBS Lett.*, Vol.168, pp.75-78, 1984.
22. A. D. MCLACHLAN and J. KARN, Periodic features in the 3-amino acid sequence of nematode myosin rod, *J. Mol. Biol.*, Vol.164, pp.605-626, 1983.

23. I. RAYMENT, W. R. Rypniewski, K. Schmidt-Bäse, R. Smith, D. R. Tomchick, M. M. Benning, D. A. Winkelmann, G. Wessenberg and H. M. Holden, Three-dimensional structure of myosin subfragment-1: A molecular motor, *Science*, Vol.261, pp.50-58, 1993.
24. H. E. HUXLEY, The mechanism of muscular contraction, *Science*, Vol.164, pp.1356-1366, 1969.
25. A. F. HUXLEY and R. M. SIMMONS, Proposed mechanism of force generation in striated muscle, *Nature*, Vol.233, pp.533-8, 1971.
26. L. SKUBISZAK, Structure and functional significance of the thick filament, *Biophysics*, Vol.41, pp.39-56, 1996.
27. K. WAKABAYASHI, M. Tokunaga, I. Kohno, Y. Sugimoto, T. Hamanaka, Y. Takezawa, T. Wakabayashi and Y. Amemiya, Small-angle synchrotron X-ray scattering reveals distinct shape changes of the myosin head during hydrolysis of ATP, *Science*, Vol.258, pp.443-447, 1992.
28. K. C. HOLMES, The swinging lever-arm hypothesis of muscle contraction, *Curr. Biol.*, Vol.7, pp.R112-8, 1997.
29. J. E. CORRIE, B. D. Brandmeier, R. E. Ferguson, D. R. Trentham, J. Kendrick-Jones, S. C. Hopkins, U. A. van der Heide, Y. E. Goldman, C. Sabido-David, R. E. Dale, S. Criddle and M. Irving, Dynamic measurement of myosin light-chain-domain tilt and twist in muscle contraction, *Nature*, Vol.400, pp.425-30, 1999.
30. H. TANAKA, K. Homma, A. H. Iwane, E. Katayama, R. Ikebe, J. Saito, T. Yanagida and M. Ikebe, The motor domain determines the large step of myosin-V, *Nature*, Vol.415, pp.192-5, 2002.
31. T. Q. UYEDA, P. D. Abramson and J. A. Spudich, The neck region of the myosin motor domain acts as a lever arm to generate movement, *Proc. Natl. Acad. Sci. USA*, Vol.93, pp.4459-64, 1996.
32. D. M. WARSHAW, W. H. Guilford, Y. Freyzon, E. Kremmentsova, K. A. Palmiter, M. J. Tyska, J. E. Baker and K. M. Trybus, The light chain binding domain of expressed smooth muscle heavy meromyosin acts as a mechanical lever, *J. Biol. Chem.*, Vol.275, pp.37167-72, 2000.
33. C. RUFF, M. Furch, B. Brenner, D. J. Manstein and E. Meyhofer, Single-molecule tracking of myosins with genetically engineered amplifier domains, *Nat. Struct. Biol.*, Vol.8, pp.226-9, 2001.
34. W. M. SHIH, Z. Gryczynski, J. R. Lakowicz and J. A. Spudich, A FRET-based sensor reveals large ATP hydrolysis-induced conformational changes and three distinct states of the molecular motor myosin, *Cell*, Vol.102, pp.683-94, 2000.
35. S. ITAKURA, H. Yamakawa, Y. Y. Toyoshima, A. Ishijima, T. Kojima, Y. Harada, T. Yanagida, T. Wakabayashi and K. Sutoh, Force-generating domain of myosin motor, *Biochem. Biophys. Res. Commun.*, Vol.196, pp.1504-10, 1993.
36. K. M. TRYBUS, E. Kremmentsova and Y. Freyzon, Kinetic characterization of a monomeric unconventional myosin V construct, *J. Biol. Chem.*, Vol.274, pp.27448-56, 1999.

37. C. PERREAULT-MICALE, A. D. Shushan and L. M. Coluccio, Truncation of a mammalian myosin I results in loss of Ca²⁺-sensitive motility, *J. Biol. Chem.*, Vol.275, pp.21618-23, 2000.
38. K. HOMMA, J. Saito, R. Ikebe and M. Ikebe, Ca(2+)-dependent regulation of the motor activity of myosin V, *J. Biol. Chem.*, Vol.275, pp.34766-71, 2000.
39. M. W. K. CHEW and J. M. SQUIRE, Packing of α -helical coiled-coil myosin rods in vertebrate muscle thick filaments, *J. Struct. Biol.*, Vol.115, pp.223-249, 1995.
40. L. SKUBISZAK and L. KOWALCZYK, The vertebrate skeletal muscle thick filaments are not three-stranded. Reinterpretation of some experimental data, *Acta Biochim Pol*, Vol.49, pp.841-53, 2002.
41. J. M. SQUIRE, General model of myosin filament structure. 2. Myosin filaments and crossbridge interactions in vertebrate striated and insect flight muscles, *J. Mol. Biol.*, Vol.72, pp.125-138, 1972.
42. J. M. SQUIRE, General models of myosin filament structure. 3. Molecular packing arrangements in myosin filaments, *J. Mol. Biol.*, Vol.77, pp.291-323, 1973.
43. J. M. SQUIRE, Architecture and function in the muscle sarcomere, *Curr. Opin. Struct. Biol.*, Vol.7, pp.247-57, 1997.
44. F. EAKINS, H. AL-Khayat, R. W. Kensler, E. P. Morris and J. M. Squire, 3D Structure of Fish Muscle Myosin Filaments, *J. Struct. Biol.*, Vol.137, pp.154-63, 2002.
45. S. EBASHI AND M. ENDO, Calcium ions and muscle contraction, *Progress in Biophysics and Molecular Biology*, Vol.18, pp.123-183, 1968.
46. E. J. O'BRIEN, J. COUCH, G. R. P. JOHNSON and E. P. MORRIES, Structure of actin and the thin filament, in C. G. dos Remedios and J. A. Barden, eds., *Actin: Structure and Function in Muscle and Non-Muscle Cells*, Academic Press, Sydney, pp.3-15, 1983.
47. K. C. HOLMES, D. Popp, W. Gebhard and W. Kabsch, Atomic model of the actin filament, *Nature*, Vol.347, pp.44-49, 1990.
48. W. KABSCHE, H. G. Mannherz, D. Suck, E. F. Pai and K. C. Holmes, Atomic structure of the actin: Dnase I complex, *Nature*, Vol.347, pp.37-44, 1990.
49. A. BREMER and U. AEBI, The structure of the F-actin filament and the actin molecule, *Curr. Biol.*, Vol.4, pp.20-26, 1992.
50. E. H. EGELMAN and A. ORLOWA, New insights into actin filament dynamics, *Curr. Opin. Struct. Biol.*, Vol.5, pp.172-180, 1995.
51. M. O. STEINMETZ, D. Stoffler, A. Hoenger, A. Bremer and U. Aebi, Actin: from cell biology to atomic detail, *J. Struct. Biol.*, Vol.119, pp.295-320, 1997.
52. J. HANSON and J. LOWY, The structure of F-actin and of actin filaments isolated from muscle, *J. Mol. Biol.*, Vol.6, pp.46-60, 1963.
53. H. E. HUXLEY and W. BROWN, The low-angle X-ray diagram of vertebrate striated muscle and its behaviour during contraction and rigor, *J. Mol. Biol.*, Vol.30, pp.383-434, 1967.

54. M. LORENZ, D. Popp and K. C. Holmes, Refinement of the F-actin model against X-ray fiber diffraction data by the use of a directed mutation algorithm, *J. Mol. Biol.*, Vol.234, pp.826-836, 1993.
55. G. N. PHILLIPS, J. P. Fillers and C. J. Cohen, Tropomyosin crystal structure and muscle regulation, *J. Mol. Biol.*, Vol.192, pp.111-127, 1986.
56. L. S. TOBACMAN, Thin filament-mediated regulation of cardiac contraction, *Annu. Rev. Physiol.*, Vol.58, pp.447-481, 1996.
57. P. F. FLICKER, G. N. Phillips, Jr. and C. Cohen, Troponin and its interactions with tropomyosin. An electron microscope study, *J. Mol. Biol.*, Vol.162, pp.495-501, 1982.
58. K. MARUYAMA, Connectin, an elastic protein of striated muscle, *Biophys. Chem.*, Vol.50, pp.73-85, 1994.
59. J. SUZUKI, S. Kimura and K. Maruyama, Electron microscopic filament lengths of connectin and its fragments, *J. Biochem.*, Vol.116, pp.406-410, 1994.
60. J. TRINICK, Titin and nebulin: protein rulers in muscle?, *J. Muscle Res. Cell Motil.*, Vol.19, pp.405-409, 1994.
61. S. LABEIT and B. KOLMERER, Titins: Giant proteins in charge of muscle ultrastructure and elasticity, *Science*, Vol.270, pp.293-296, 1995.
62. B. KOLMERER, N. Olivieri, C. C. Witt, B. G. Herrmann and S. Labeit, Genomic organization of M line titin and its tissue-specific expression in two distinct isoforms, *J. Mol. Biol.*, Vol.256, pp.556-563, 1996.
63. S. LABEIT, M. Gautel, A. Lakey and J. Trinick, Towards a molecular understanding of titin, *EMBO*, Vol.11, pp.1711-1716, 1992.
64. K. WANG, J. Wright and R. Ramirez-Mithell, Architecture of the titin/nebulin containing cytoskeletal lattice of the striated muscle sarcomere-evidence of elastic and inelastic domains of the bipolar filaments, *J. Cell Biol.*, Vol.99, pp.435, 1984.
65. Y. ITOH, S. T. Kimura, S. Ohashi, K. Higuchi, H. Sawada, H. Shimizu, T. Shibata and M. Maruyama, Extensible and less-extensible domains of connection filaments in stretched vertebrate skeletal muscle as detected by immunofluorescence and immunoelectron microscopy using monoclonal antibodies, *J. Biochem.*, Vol.104, pp.504-508, 1988.
66. A. WHITING, J. Wardate and J. Trinick, Does titin regulate the length of muscle thick filaments?, *J. Mol. Biol.*, Vol.205, pp.263-268, 1989.
67. D. O. FÜRST, R. Nave, M. Osborn and K. Weber, Repetitive titin epitopes with a 42 nm spacing coincide in relative position with known A-band striations also identified by major myosin-associated proteins: an immunoelectro-microscopical study on myofibrils, *J. Cell Sci.*, Vol.94, pp.119-125, 1989.
68. K. TROMBITAS, G. H. Pollack, J. Wright and K. Wang, Elastic properties of titin filaments demonstrated using a "freeze- break" technique, *Cell Motil. Cytoskeleton*, Vol.24, pp.274-83, 1993.
69. K. TROMBITAS and G. H. POLLACK, Elastic properties of connecting filaments along the sarcomere, *Adv. Exp. Med. Biol.*, Vol.332, pp.71-9, 1993.

70. A. M. GORDON, A. F. Huxley and F. J. Julian, The variation in isometric tension with sarcomere length in vertebrate muscle fibres, *J. Physiol.*, Vol.184, pp.170-192, 1966.
71. L. SKUBISZAK, Mechanism of muscle contraction, *Technology and Health Care*, Vol.1, pp.133-142, 1993.
72. L. SKUBISZAK and L. KOWALCZYK, Relation between the mechanical properties of muscles and their structure on the molecular level, *Eng. Trans.*, Vol.49, pp.191-212, 2001.
73. L. SKUBISZAK, Force generation in muscle. Organization in working structures of muscle, *Lect. Not. ICB Sem.*, Vol.5, pp.237-297, 1989.
74. E. J. O'BRIEN, P. Bennett and J. Hanson, Optical diffraction studies of myofibrillar structure, *Philosophical Transactions of the Royal Society of London*, Vol.160/B, pp.201-208, 1971.
75. E. J. O'BRIEN, J. Gillis and J. Couch, Symmetry and molecular arrangement in paracrystals of reconstituted muscle thin filaments, *J. Mol. Biol.*, Vol.99, pp.461-475, 1975.
76. T. WAKABAYASHI, H. E. Huxley, L. A. Amos and A. Klug, Three-dimensional image reconstruction of actin-tropomyosin complex and actin-tropomyosin-troponin-troponin I complex, *J. Mol. Biol.*, Vol.93, pp.477-479, 1975.
77. D. A. D. PARRY, Movement of tropomyosin during regulation of vertebrate skeletal muscle: simple physical model, *Biochem. Biophys. Res. Commun.*, Vol.68, pp.323-328, 1976.
78. M. KRESS, H. E. Huxley, A. Faruqi and J. Hendrix, Structural changes during activation of frog muscle studied by time-resolved X-ray diffraction, *J. Mol. Biol.*, Vol.188, pp.325-342, 1986.
79. P. VIBERT, R. Craig and W. Lehman, Steric-model for activation of muscle thin filaments, *J. Mol. Biol.*, Vol.266, pp.8-14, 1997.
80. K. WAKABAYASHI, Y. Sugimoto, H. Tanaka, Y. Ueno, Y. Takezawa and Y. Amemiya, X-ray diffraction evidence for the extensibility of actin and myosin filaments during muscle contraction, *J. Biophys.*, Vol.67, pp.2422-2435, 1994.
81. L. SKUBISZAK and L. KOWALCZYK, Computer system modelling muscle work, *Technology and Health Care*, Vol.6, pp.139-149, 1998.
82. L. KOWALCZYK and L. SKUBISZAK, Algorithm for fast calculation of mass distribution, *Biocyb. Biomed. Engin.*, Vol.19, pp.31-38, 1999.
83. R. CRAIG and W. LEHMAN, Crossbridge and tropomyosin positions observed in native, interacting thick and thin filaments, *J. Mol. Biol.*, Vol.311, pp.1027-36, 2001.
84. R. C. GONZALEZ and P. WINTZ, Image transforms, *Digital image processing*, Addison-Wesley Publishing Company, Massachusetts, pp.61-137, 1987.
85. A. KLUG, F. Crick and H. W. Wyckoff, Diffraction by helical structures, *Acta Cryst.*, Vol.11, pp.199-212, 1958.
86. R. J. C. LEVINE, Differences in myosin head arrangement on relaxed thick filaments from *Lethocerus* and rabbit muscles, *J. Muscle Res. Cell Motil.*, Vol.18, pp.529-543, 1997.

87. S. XU, S. MALINCHIK, D. GILROY, T. KRAFT, B. BRENNER, L. C. YU, X-ray diffraction studies of cross-bridges weakly bound to actin in relaxed skinned fibers of rabbit psoas muscle, *J. Biophys.*, Vol.73, pp.2292-2303, 1997.
88. L. HUDSON, J. J. HARFORD, R. C. DENNY, J. M. SQUIRE, Myosin head configuration in relaxed fish muscle: Resting state myosin heads must swing axially by up to 150 or turn upside down to reach rigor, *J. Mol. Biol.*, Vol.273, pp.440-455, 1997.

